SUPPORTING INFORMATION

Chemical interrogation of LuxR-type proteins reveals new insights into quorum sensing receptor selectivity and the potential for interspecies bacterial signaling

Joseph P. Gerdt,[†,a] Danielle M. Wittenwyler (née Stacy),[†] Joshua B. Combs, Michelle E. Boursier, Jacob W. Brummond, He Xu, and Helen E. Blackwell[*]

Department of Chemistry, University of Wisconsin–Madison, 1101 University Ave., Madison, WI 53706, USA

CONTENTS.

[†] These authors contributed equally to this work.
[a] *Current address*: *Department of Biological Chemistry and Molecular Pharmacology, Harvard Medical School, Boston, MA 02115, USA*
[*] To whom correspondence should be addressed: blackwell@chem.wisc.edu; 608-262-1503

EXPERIMENTAL METHODS

General methods

All chemical reagents were purchased from commercial sources (Alfa-Aesar, Sigma-Aldrich, and Acros) and used without further purification. Solvents were purchased from commercial sources (Sigma-Aldrich and J.T. Baker) and used as obtained, with the exception of dichloromethane (CH_2Cl_2), which was distilled over calcium hydride immediately prior to use. Water was purified using a Millipore Analyzer Feed System.

Nuclear magnetic resonance (NMR) spectra were recorded in deuterated solvents on a Varian MercuryPlus 300 MHz spectrometer or Bruker Avance III 500 MHz spectrometer. Chemical shifts are reported in parts per million (ppm, δ) using corresponding solvents or tetramethylsilane (TMS) as a reference. Couplings are reported in hertz (Hz). Electrospray ionization mass spectrometry (MS) measurements were performed on a Waters LCT instrument. Samples were dissolved in acetonitrile and sprayed with a sample cone voltage of 20.

Reversed-phase high performance liquid chromatography (RP-HPLC) was performed using a Shimadzu system equipped with an SCL-10Avp controller, an LC-10AT pump, an FCV-10ALvp solvent mixer, and an SPD-10MAvp UV/vis diode array detector. A Restek Premier C18 column (5 μm, 4.6 mm x 250 mm) was used for all analytical RP-HPLC work. An Agilent Zorbax prepHT 300SB-C18 column (7 μm, 21.2 mm x 250 mm) was used for all preparative RP-HPLC work. Standard RP-HPLC conditions were as follows: flow rates were 1 mL min^{-1} for analytical separations and 9 mL min^{-1} for preparative separations; mobile phase A = water; mobile phase B = acetonitrile.

Compound synthesis

AHLs **9**, **11**–**15**, **20**, **22**, **23**, and **26** were synthesized and purified by RP-HPLC for this study according to our previously reported protocols (purities >95%).[1-5] AHLs that have been reported previously (**1**–**8**, **10**, **16**–**19**, **21**, **24**, and **25**) are listed in **Table S1** with original compound names and original citations. AHLs **9**, **11**–**14**, and **20** are all commercially available (Cayman Chemical #10011200; Sigma Aldrich #61698, #68873, #53727, #51481; Chemodex #O0061), and our

samples synthesized in-house yielded characterization data that matched those of commercial samples. Compound characterization data for the new AHLs in this study (**15**, **22**, **23**, and **26**) are provided at the end of this document.

Biological reagents and strain information

All biological reagents were purchased from Fisher Scientific and used according to enclosed instructions. Luria-Bertani (LB) medium was prepared as instructed with pH = 7.0. Buffers and solutions (Z buffer, 0.1% (m/v) aqueous SDS, and phosphate buffer) for Miller absorbance assays were prepared as described.[6] The *A. baumannii* M2 *abaI::lacZ* (*ΔabaI* reporter) strain was used for the AbaR bacteriological assay in this study.[7] The *E. coli* DH5α [F^- ϕ80d*lacZ*Δ*M15* Δ(*lacZYA-argF*)*U169 deoR recA1 endA1 hsdR17*(r_K^- m_K^+) *phoA supE44* λ^- *thi-1 gyrA96 relA1*] strain harbouring a LasR expression vector (pJN105L) and a plasmid-born *lasI–lacZ* fusion (pSC11) was used for the LasR bacteriological assay in this study.[8] Bacterial cultures were grown in a standard laboratory incubator at 37 °C with shaking (200 rpm) unless noted otherwise. Absorbance measurements were obtained using a Biotek Synergy 2 microplate reader using Gen5 data analysis software. All bacteriological reporter assays were performed in triplicate. No AHL was found to inhibit growth over the time course of the assays in this study.

Compound handling

Stock solutions of synthetic compounds (10 mM and 1 mM) were prepared in DMSO and stored at 4 °C in sealed vials. The amount of DMSO used in small molecule screens did not exceed 2% (v/v). Solvent resistant polypropylene or polystyrene 96-well multititer plates were used when appropriate for small molecule screening. The concentrations of synthetic AHL ligand used in the primary antagonism and agonism assays and the relative ratios of synthetic ligand to **1** (10 μM : 10 nM) and **2** (100 μM: 0.70 μM) in the LasR and AbaR antagonism assays, respectively, were chosen to provide the greatest dynamic range between inhibitors and activators for each bacterial reporter strain. The concentration of **1** was twice its EC_{50} value in the *E. coli* reporter strain. The concentration of **2** was equal to its EC_{50} value in the *A. baumannii* (*ΔabaI*) reporter strain.[9]

AbaR reporter gene assay (β-galactosidase)

For primary agonism assays, 2 μL of concentrated control or AHL stock solution (to give a final concentration of 100 μM) was added to wells in a 96-well multititer plate. An overnight culture of the *A. baumannii* (*ΔabaI*) reporter strain (OD_{600} = 1.2) was diluted 1:100 with fresh LB medium. A 198-μL portion of the diluted culture was added to each well of the multititer plate containing AHLs. Plates were incubated statically at 37 °C for 18–24 h. The cultures were then assayed for β-galactosidase activity following the standard Miller assay method that we previously reported for this strain.[6, 9] Briefly, the OD_{600} of each well of the 96-well multititer plate was recorded. Next, 50 μL aliquots from each well were transferred to a solvent resistant 96-well multititer plate containing 200 μL Z buffer, 8 μL $CHCl_3$, and 4 μL 0.1%(w/v) aqueous SDS. This suspension was mixed via repetitive pipetting (30x), after which the $CHCl_3$ was allowed to settle. A 150-μL aliquot from each well was transferred to a fresh 96-well multititer plate, 20 μL of *ortho*-nitrophenyl-β-galactoside substrate (ONPG, 4 μg mL^{-1} in phosphate buffer) was added to each well at time zero, and the plate was incubated at 55 °C for 20 min. Thereafter, the enzymatic reaction was terminated by the addition of 50 μL of 1 M Na_2CO_3. Absorbance at 420 and 550 nm were measured for each well using a plate reader, and Miller units were calculated according to standard methods.[8] Primary AbaR antagonism assays were performed in a similar manner except that the synthetic AHL was screened at 100 μM against 0.70 μM **2**. Dose-response assays were performed identically to primary screens, but used a range of AHL concentrations (200 pM – 200 μM for agonism and 10 nM – 100 μM for antagonism).

LasR reporter gene assay (β-galactosidase)

An overnight culture of the *E. coli* LasR reporter was diluted 1:10 with fresh LB medium containing 100 μg mL^{-1} ampicillin and 15 μg mL^{-1} gentamicin. The subculture was incubated with shaking at 37 °C until the optical density of 200 μL reached 0.27 (approximately 90 min). Arabinose (4 mg mL^{-1}) was then added to the culture to induce production of LasR. A 198-μL portion of the diluted culture was added to each well of a multititer plate containing AHLs prepared in the same way outlined above. Plates were incubated statically at 37 °C until the

optical density of the wells reach 0.45 (approximately 2 h). The cultures were then assayed for β-galactosidase activity according to the method described above for AbaR.

Sequence alignment

The ClustalW sequence alignment displayed in **Fig. 3D** and **Table S2** was performed with the BLOSUM cost matrix in Geneious software (Biomatters Ltd, New Zealand). Species names and GenBank Accession numbers for the aligned sequences are as follows: AbaR, *A. baumannii*, EGJ67179.1; TraR, *A. tumefaciens*, AAC28121.1; LasR, *P. aeruginosa*, AAG04819.1; QscR, *P. aeruginosa*, NP_250589.1.

SUPPLEMENTARY FIGURES

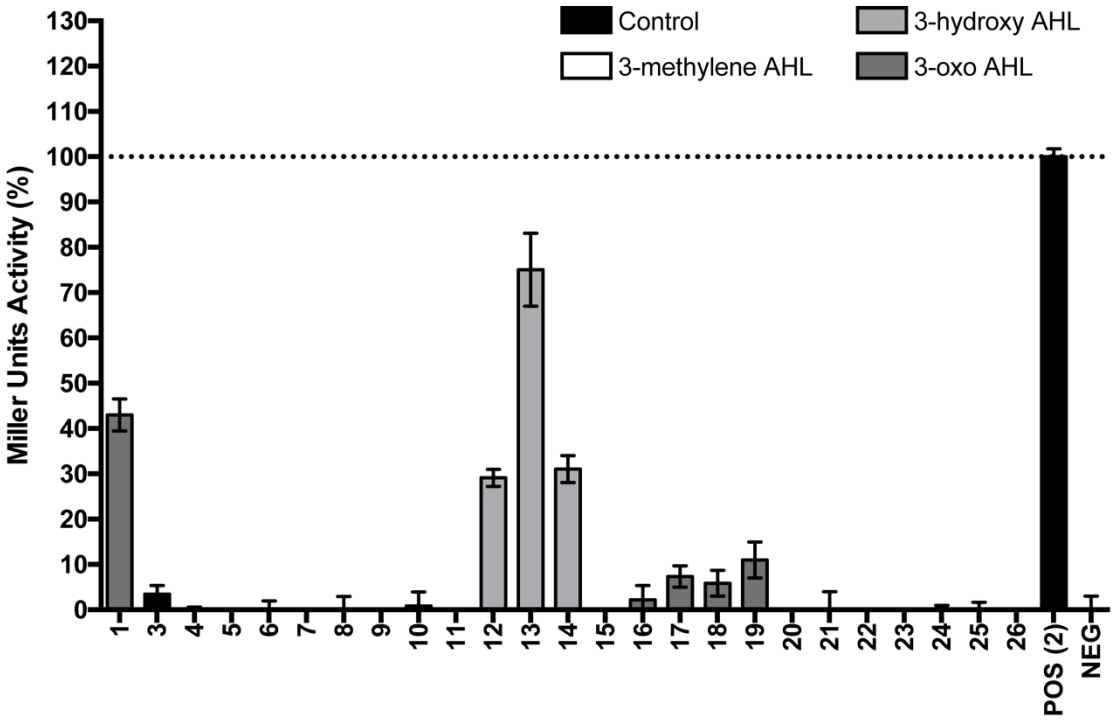

Fig. S1 Primary AbaR agonism screening data for the control compounds and non-native AHLs in the *A. baumannii* (*ΔabaI*) reporter strain. Ligands were screened at 100 μM. Positive control (POS) = 100 μM (*R*)-OH-dDHL **(2)**. Negative control (NEG) = DMSO without compound. Miller units report relative absorbance. Error bars in each plot indicate standard error of the mean of nine values.

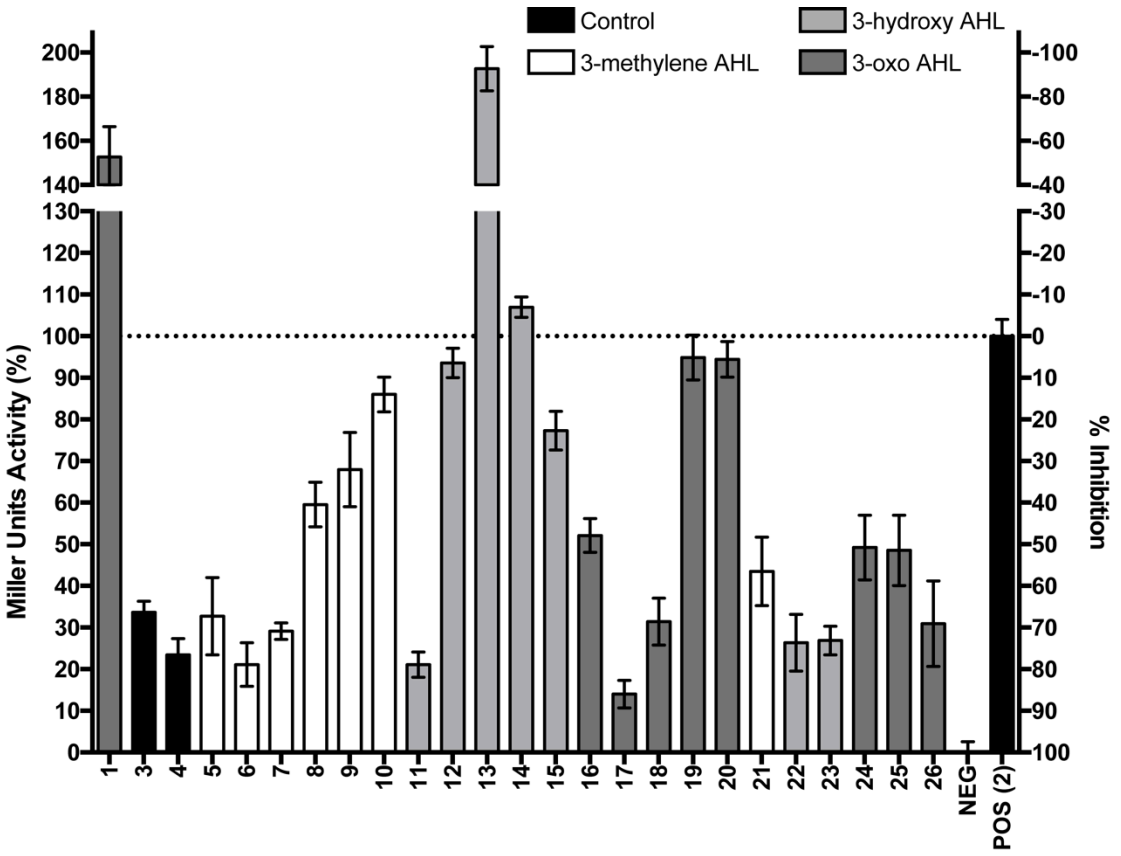

Fig. S2 Primary AbaR antagonism screening data for the control compounds and non-native AHLs in the *A. baumannii* (*ΔabaI*) reporter strain. Compounds were screened at 100 μM against 700 nM **2**. Positive control (POS) = 700 nM **2**. Negative control (NEG) = DMSO without compound. Miller units report relative absorbance. Error bars in each plot indicate standard error of the mean of nine values.

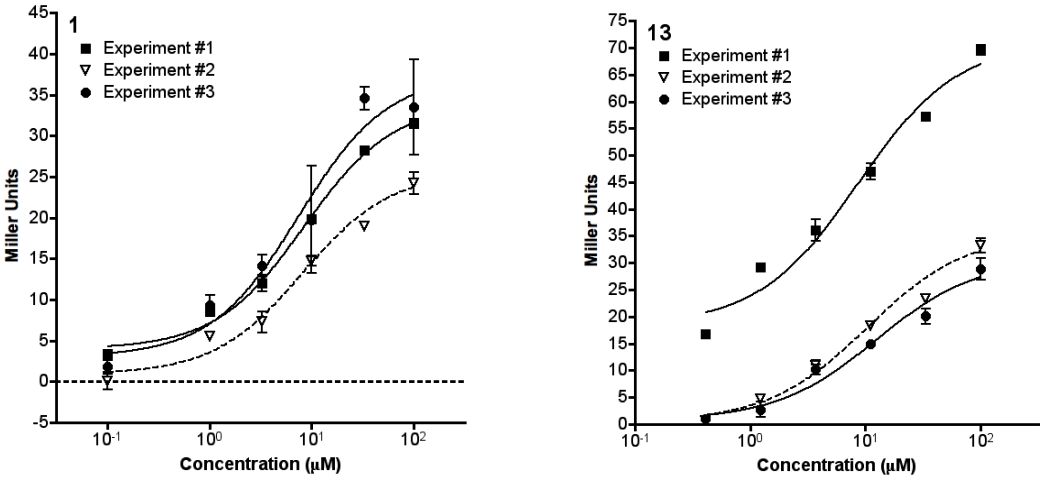

Fig. S3 AbaR agonism dose response curves for AHLs **1** and **13** in the *A. baumannii* (*ΔabaI*) reporter strain. Compounds screened over varying concentrations. Each plot labeled with compound number at top left. Miller units report relative absorbance. Error bars indicate standard error of the mean of triplicate values.

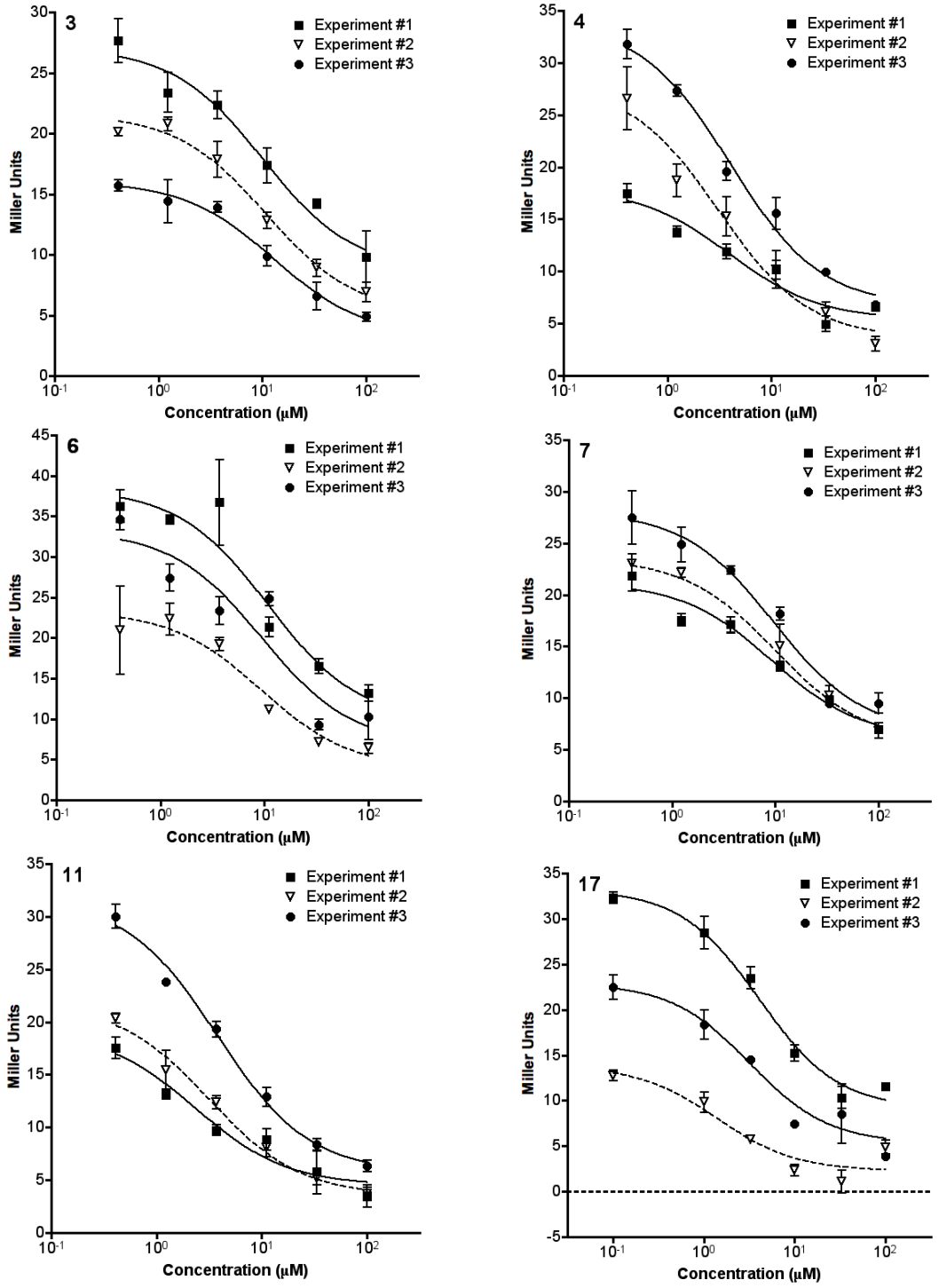

Fig. S4 AbaR antagonism dose response curves for AHLs **3**, **4**, **6**, **7**, **11**, and **17** in the *A. baumannii (ΔabaI)* reporter strain. Compounds screened against 700 nM **2** over varying concentrations. Each plot labeled with compound number at top left. Miller units report relative absorbance. Error bars indicate standard error of the mean of triplicate values.

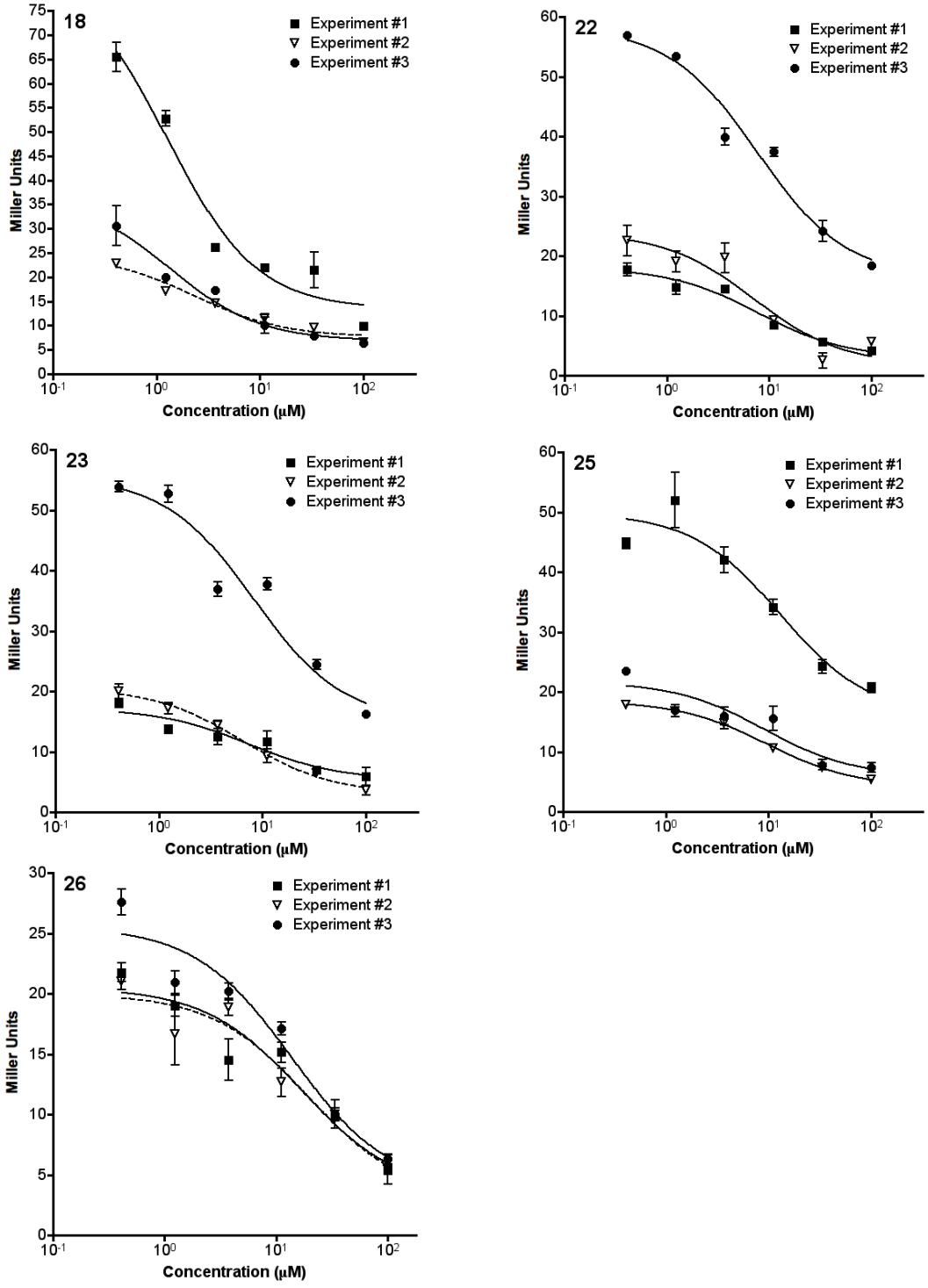

Fig. S5 AbaR antagonism dose response curves for AHLs **18**, **22**, **23**, **25**, and **26** in the *A. baumannii (ΔabaI)* reporter strain. Compounds screened against 700 nM **2** over varying concentrations. Each plot labeled with compound number at top left. Miller units report relative absorbance. Error bars indicate standard error of the mean of triplicate values.

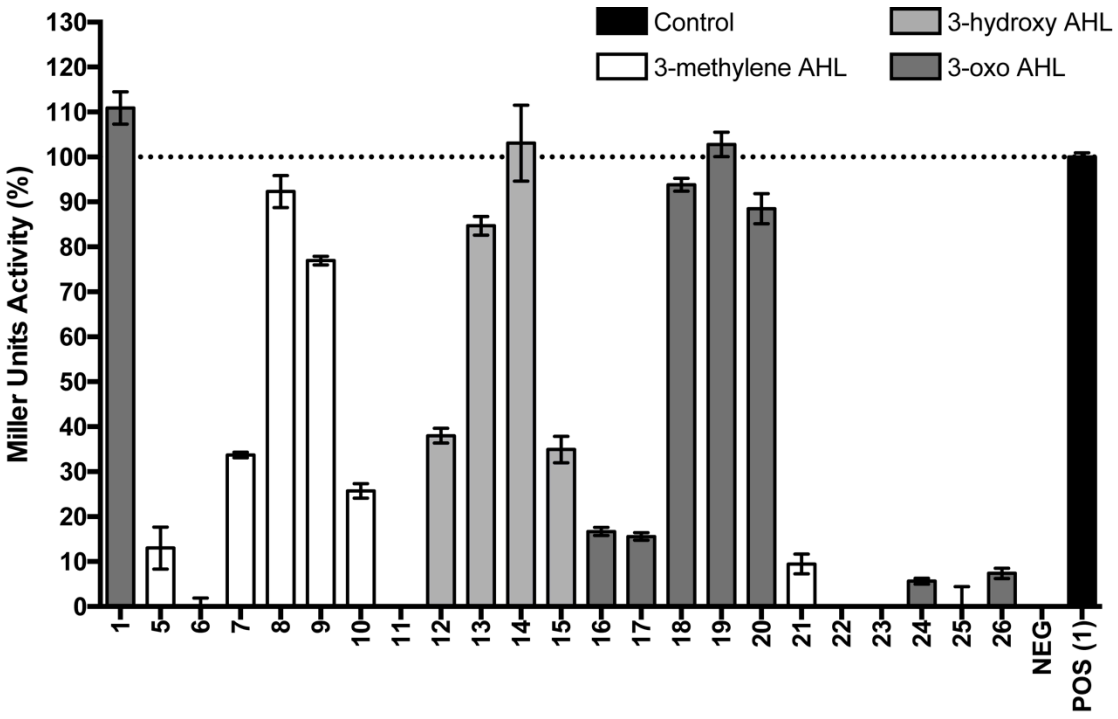

Fig. S6 Primary LasR agonism screening data for the control compounds and non-native AHLs in the *E. coli* pJN105L reporter strain. Compounds screened at 10 μM. Positive control (POS) = 10 μM OdDHL (**1**). Negative control (NEG) = DMSO without compound. Miller units report relative absorbance. Error bars in each plot indicate standard error of the mean of nine values.

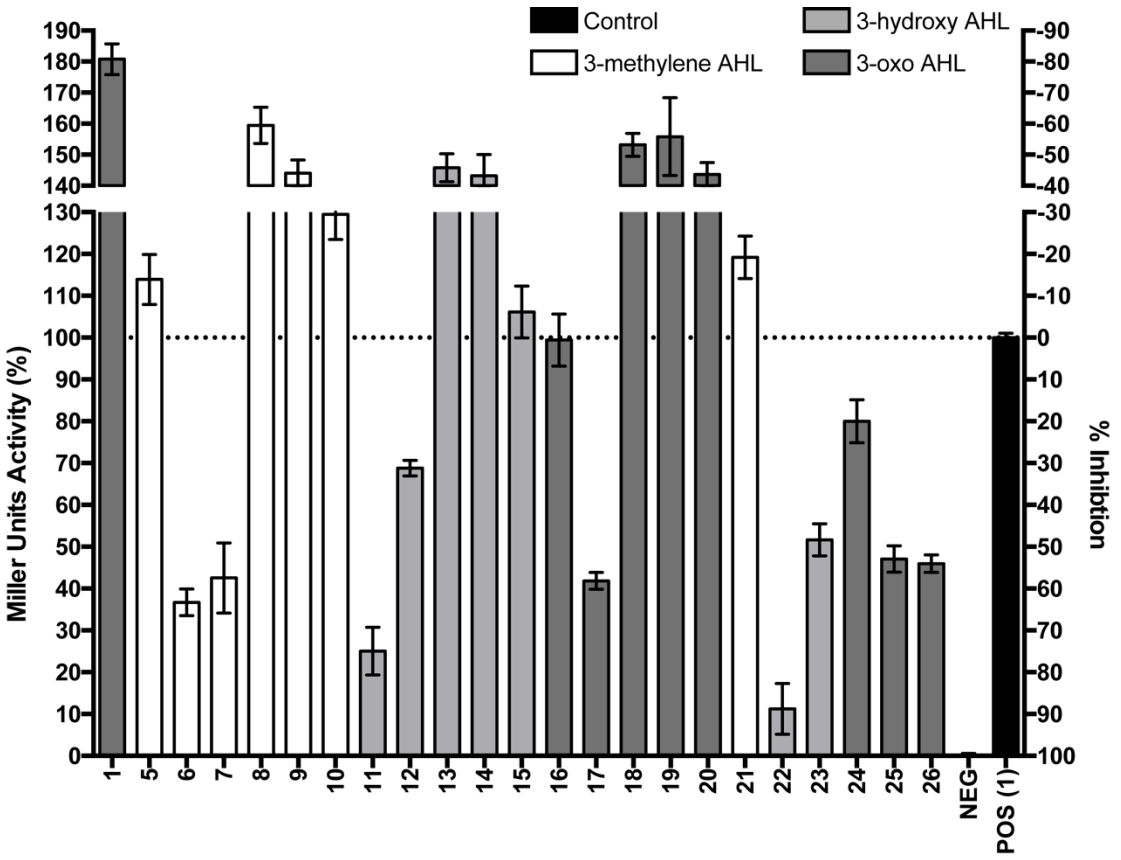

Fig. S7 Primary LasR antagonism screening data for the control compounds and non-native AHLs in the *E. coli* pJN105L reporter strain. Compounds tested at 10 μM against 10 nM **1**. Positive control (POS) = 10 nM **1**. Negative control (NEG) = DMSO without compound. Miller units report relative absorbance. Error bars in each plot indicate standard error of the mean of nine values.

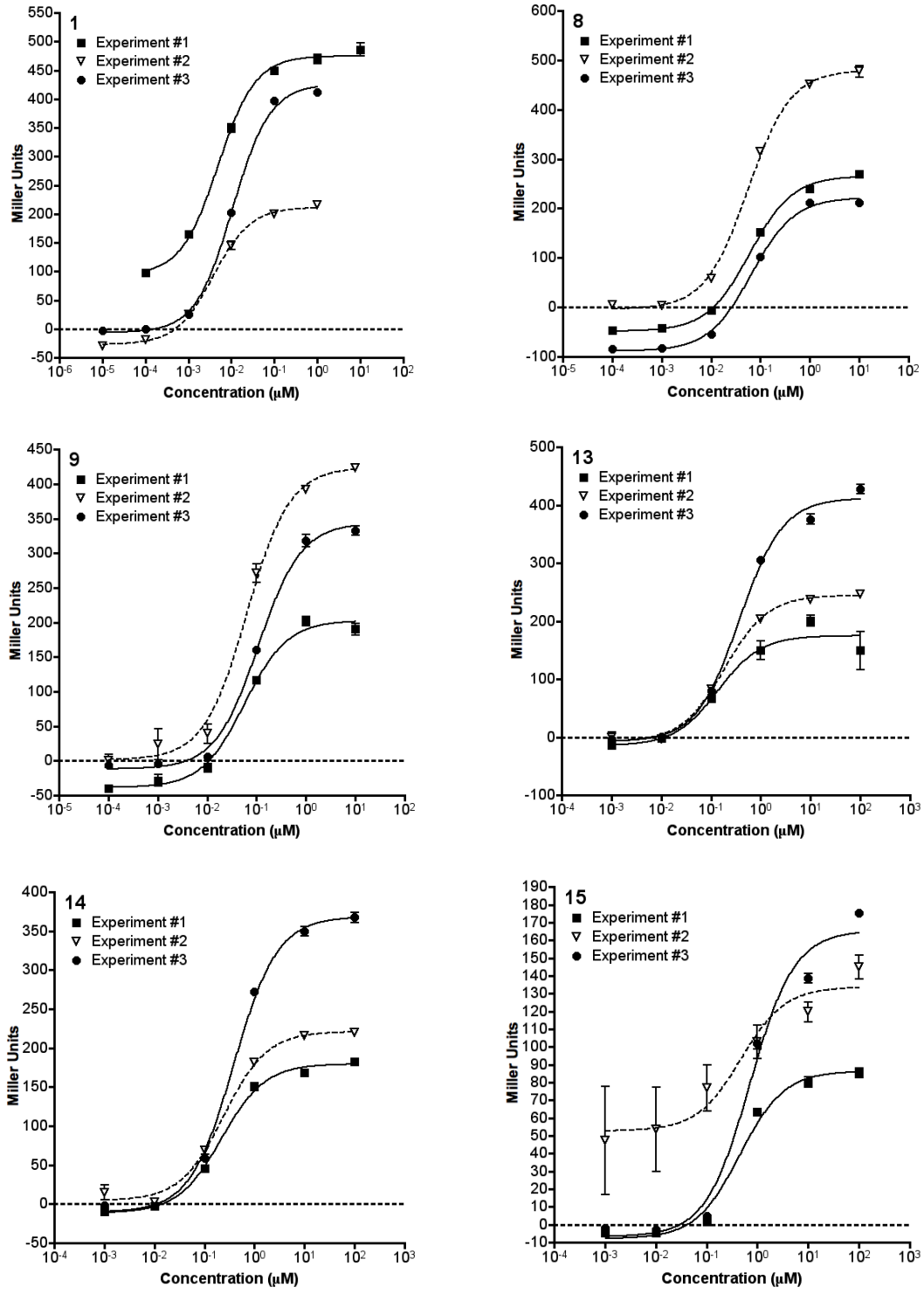

Fig. S8 LasR agonism dose response curves for AHLs **1**, **8**, **9**, and **13–15** in the *E. coli* pJN105L reporter strain. Compounds screened over varying concentrations. Each plot labeled with compound number at top left. Miller units report relative absorbance. Error bars indicate standard error of the mean of triplicate values.

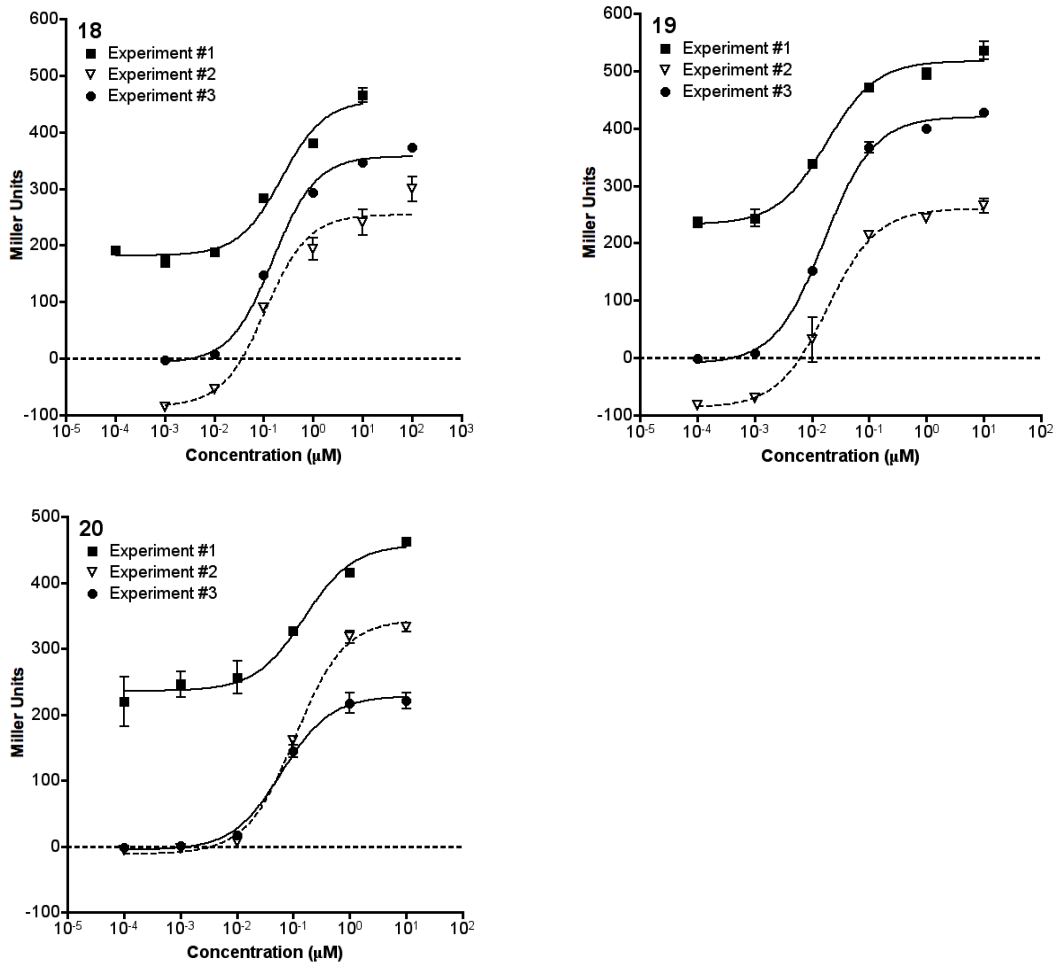

Fig. S9 LasR agonism dose response curves for AHLs **18**–**20** in the *E. coli* pJN105L reporter strain. Compounds screened over varying concentrations. Each plot labeled with compound number at top left. Miller units report relative absorbance. Error bars indicate standard error of the mean of triplicate values.

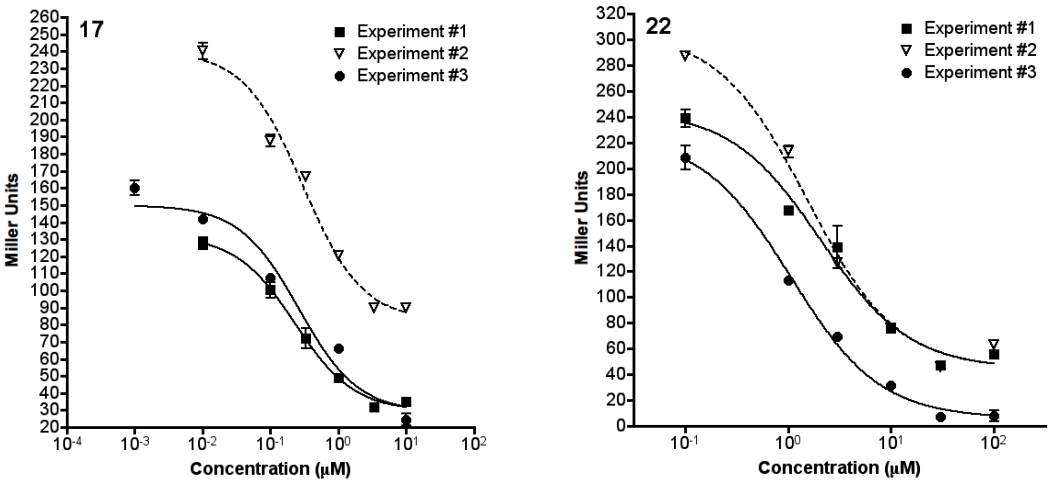

Fig. S10 LasR antagonism dose response curves for AHLs **17** and **22** in the *E. coli* pJN105L reporter strain. Compounds screened against 10 nM **1** over varying concentrations. Each plot labeled with compound number at top left. Miller units report relative absorbance. Error bars indicate standard error of the mean of triplicate values.

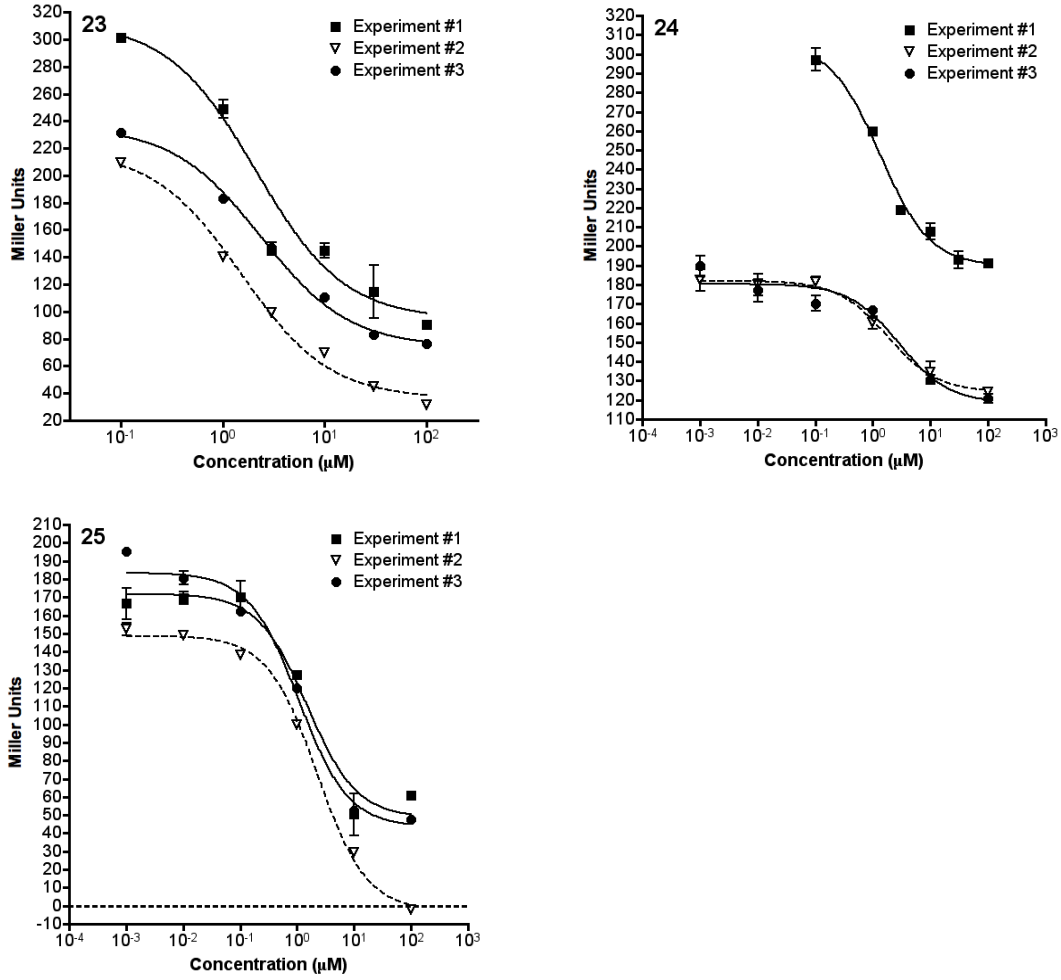

Fig. S11 LasR antagonism dose response curves for AHLs **23–25** in the *E. coli* pJN105L reporter strain. Compounds screened against 10 nM **1** over varying concentrations. Each plot labeled with compound number at top left. Miller units report relative absorbance. Error bars indicate standard error of the mean of triplicate values.

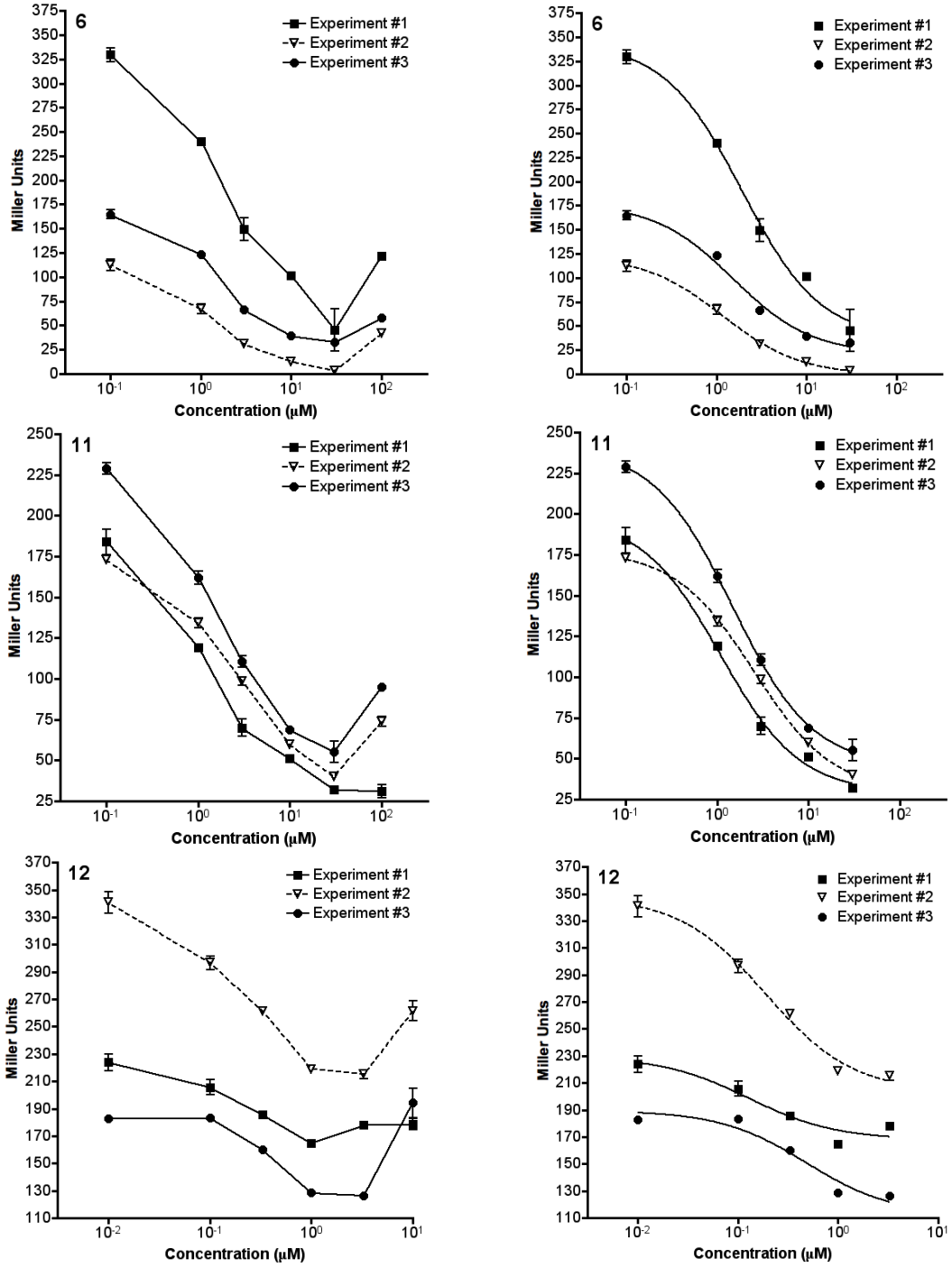

Fig. S12 LasR antagonism dose response curves for AHLs **6**, **11**, and **12** in the *E. coli* pJN105L reporter strain. Full antagonism dose response curves (left) and portions of curves used to calculate IC_{50} values (right). Compounds screened against 10 nM **1** over varying concentrations. Each plot labeled with compound number at top left. Miller units report relative absorbance. Error bars indicate standard error of the mean of triplicate values.

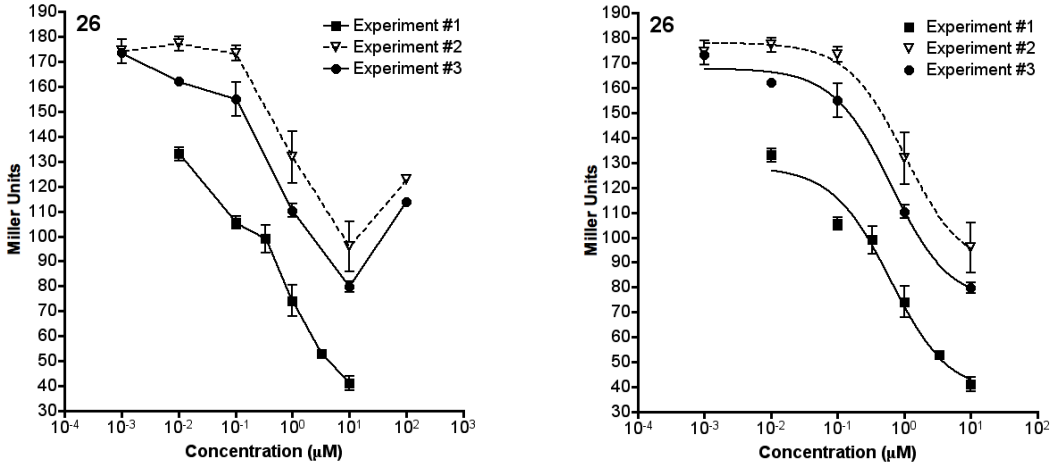

Fig. S13 LasR antagonism dose response curves for AHL **26** in the *E. coli* pJN105L reporter strain. Full antagonism dose response curves (left) and portions of curves used to calculate IC_{50} value (right). Compound screened against 10 nM **1** over varying concentrations. Each plot labeled with compound number at top left. Miller units report relative absorbance. Error bars indicate standard error of the mean of triplicate values.

SUPPLEMENTARY TABLES

Table S1 Listing of AHLs in this study with original compound names and citations.

AHL name (as described here)	AHL name (as previously reported)	Original citation
1	**2** (OdDHL)[a]	[1,2]
2	*(R)*-OH-dDHL	[3]
3	**C6**	[1,2]
4	**C11**	[1,2]
5	**A2**[a]	[1,2]
6	**A3**[a]	[1,2]
7	**A4**[a]	[1,2]
8	**A5**[a]	[1,2]
9	-[a]	This study
10	**A6**[a]	[1,2]
11	-[a]	This study
12	-[a]	This study
13	-[a]	This study
14	-[a]	This study
15	-	This study
16	**3**[a]	[1,2]
17	**1**[a]	[1,2]
18	**A7**[a]	[1,2]
19	**A8**[a]	[1,2]
20	-[a]	This study
21	**6**	[1,2]
22	-	This study
23	-	This study
24	**5**	[1,2]
25	**15**	[10]
26	-	This study

[a] Commercially available AHLs. Our samples synthesized in-house yielded characterization data that matched those of commercial samples.

Table S2 Tested AHLs and a selection of their known cognate bacteria.

Acyl Chain	AHL	Producing bacterial species	Reference
3-methylene			
C_6	**5**	*Chromobacterium violaceum, Ralstonia solanacearum,* and *Pseudomonas fluorescens*	11-13
C_8	**6**	*Burkholderia cepacia* and *R. solanacearum*	12, 14
C_{10}	**7**	*Sinorhizobium meliloti* and *P. fluorescens*	13, 15
C_{12}	**8**	*Aeromonas hydrophila, Aeromonas salmonicida, Pseusomonas aeruginosa, Yersinia enterocolitica, P. fluorescens,* and *Serratia liquefaciens*	16
C_{14}	**9**	*S. meliloti, A. hydrophila, A. salmonicida, Y. enterocolitica,* and *Rhodobacter capsulatus*	15-17
C_{16}	**10**	*R. capsulatus, Paracoccus denitrificans, Agrobacterium vitis,* and *S. meliloti*	15, 17-19
3-hydroxyl			
C_8	**11**	*Aeromonas culicicola 3249T, Burkholderia thailandensis,* and *Burkholderia mallei*	20, 21
C_{10}	**12**	*Phaeobacter gallaeciensis T5* and *B. thailandensis*	20, 22, 23
C_{12}	**13**	*Acinetobacter baumannii*	7
C_{14}	**14**	*Pseudomonas cedrina*	24
C_{16}	**15**	None reported	
3-oxo			
C_6	**16**	*Vibrio fischeri, Pectobacterium carotovora, Serratia proteamaculans B5a, Pseudomonas putida,* and *Rahnella aquatilis*	25, 26
C_8	**17**	*Agrobacterium tumefaciens, P. putidia, R. aquatilis,* and *Pseudonomas syringae*	24, 26, 27
C_{10}	**18**	*Vibrio anguillarum, Pantoea agglomerans, P. fluorescens PF7,* and *P. putida*	24, 26, 28
C_{12}	**1**	*P. aeruginosa*	29
C_{14}	**19**	*P. aeruginosa strain MW3A, R. aquatilis, P. fluorescens,* and *S. meliloti*	18, 24, 30
C_{16}	**20**	*A. vitis, Pseudomonas sp.,* and *S. meliloti*	18, 19 31

Table S3 AbaR and LasR primary agonism and antagonism assay data and EC_{50} and IC_{50} values with confidence intervals for the aliphatic-tail AHLs (**1**, **2**, and **5**–**20**)[a]

Acyl Chain	AHL	Activation (%)[b]	EC_{50} value (μM)[c]	Inhibition (%)[d]	IC_{50} value (μM)[e]
AbaR					
(R)-OH-dDHL	**2**	100	0.699		
3-methylene					
C_6	**5**	0		67	
C_8	**6**	0		79	9.87 (8.28–11.8)
C_{10}	**7**	0		71	9.64 (8.94–10.4)
C_{12}	**8**	0		40	
C_{14}	**9**	0		32	
C_{16}	**10**	1		14	
3-hydroxyl					
C_8	**11**	0		79	3.06 (1.91–4.90)
C_{10}	**12**	29		6	
C_{12}	**13**	75	10.3 (7.18–14.7)[f]	–93	
C_{14}	**14**	31		–7	
C_{16}	**15**	0		23	
3-oxo					
C_6	**16**	2		48	
C_8	**17**	7		86	2.65 (0.892–7.90)
C_{10}	**18**	6		69	1.60 (0.826–3.09)
C_{12}	**1**	43	7.53 (5.92–9.59)[f]	–53	
C_{14}	**19**	11		5	
C_{16}	**20**	0		6	

Acyl Chain	AHL	Activation (%)[b]	EC_{50} value (nM)[c]	Inhibition (%)[d]	IC_{50} value (μM)[e]
LasR					
OdDHL	**1**	100	5.79 (2.04–16.4)		
3-methylene					
C_6	**5**	13		–14	
C_8	**6**	0		63	1.29 (0.961–1.74)[g]
C_{10}	**7**	34		57	
C_{12}	**8**	92	59.6 (51.4–69.0)	–59	
C_{14}	**9**	77	72.2 (36.7–142)[f]	–44	
C_{16}	**10**	26		–29	
3-hydroxyl					
C_8	**11**	0		75	1.60 (0.686–3.73)[g]
C_{10}	**12**	38		31	0.112 (0.0748–0.168)[g]
C_{12}	**13**	85	248 (124–495)[f]	–46	
C_{14}	**14**	103	270 (149–487)	–43	
C_{16}	**15**	35	511 (294–889)[f]	–6	
3-oxo					
C_6	**16**	17		1	
C_8	**17**	16		58	0.260 (0.199–0.339)
C_{10}	**18**	94	154 (73.4–323)	–53	
C_{12}	**1**	100	5.79 (2.04–16.4)	–81	
C_{14}	**19**	103	17.5 (15.4–19.8)	–56	
C_{16}	**20**	88	105 (40.1–275)[f]	–44	

[a] All assays performed in biological triplicate. [b] AHLs evaluated at 100 μM and normalized to **2** at 100 μM for AbaR, and evaluated at 10 μM and normalized to **1** at 10 μM for LasR. Errors displayed in **Fig. 2**. [c] EC_{50} values determined by testing AHLs over a range of concentrations. 95% confidence intervals displayed. [d] AHLs evaluated at 100 μM against **2** at 700 nM for AbaR and evaluated at 10 μM against **1** at 10 nM for LasR. Errors displayed in **Fig. 2**. Negative values indicate agonistic activity. [e] IC_{50} values determined by testing AHLs over a range of concentrations against **2** at 700 nM for AbaR and against **1** at 10 nM for LasR. 95% confidence intervals displayed. [f] Dose response curve reached a plateau over concentrations tested, yet the level of the maximal induction was lower than that for **2** for AbaR or **1** for LasR. [g] Dose response curve upturned at higher concentrations and did not reach 100% inhibition over concentrations tested (prior to upturn); IC_{50} value calculated from partial antagonism dose response curve reported in **Fig. S12** and **Fig. S13**.

Table S4 Full version of sequence alignment displayed in Fig. 3 in the main text. See Fig. 3 for details. Key residues are boxed.

```
         1       10        20        30        40        50        60        70        80        90       100       110       120       130
         |        |         |         |         |         |         |         |         |         |         |         |         |         |
AbaR     MESWQEDLLSAFLVVKNEYQLFDIVKSTASRLGFDYCAYGMQSPLSIAEPKTIMLNNYPEAWQKRYVEGQYVKIDPTVQHCMVSLQPLVWSSQSA---KTQAEKDFWEEARSYGLNVGWAQSSRDFIGTR
TraR     MQHWLDKLTDLAAIEGDECILKTGLADIADHFGFTGYAY-----LHIQHRHITAVTNYHRQWQSTYFDKKFEALDPVVKRARSRKHIFTWSGEHERPTLSKDERAFYDHASDFGIRSGITIPIKTANGFM
LasR     -MALVDGFLELE-RSSGKLEWSAILQKMASDLGFSKILFGLLPKDSQDYENAFIVGNYPAAWREHYDRAGYARVDPTVSHCTQSVLPIFWEPSIY---QTRKQHEFFEEASAAGLVYGLTMPLHGARGEL
QscR     MHDEREGYLEILSRITTEEEFFSLVLEICGNYGFEFFSFGARAPFPLTAPKYHFLSNYPGEWKSRYISEDYTSIDPIVRHGLLEYTPLIWNGE-----DFQENRFFWEEALHHGIRHGWSIPVRGKYGLI

                140       150       160       170       180       190       200       210       220       230       240
                 |         |         |         |         |         |         |         |         |         |         |
AbaR     GMLTLARSNDQLSEK-EQKAQYTNMYWLTQTVHSSIAKIVNDVEFAKFNLYLTNREKEALRWTAEGKTSAEIAQILGVTERTVNFHLSNSMQKLNVNNKISAAIRAVMLGLL--
TraR     SMFTMASDKPVIDLD-REIDAVAAAATIGQIHARIS--FLRTTPTAEDAAWLDPKEATYLRWIAVGKTMEEIADVEGVKYNSVRVKLREAMKRFDVRSKAHLTALAIRRKLI--
LasR     GALSLSVEAENRAEANRFMESVLPTLWMLKDYALQSGAGLAFEHPVSKPVVLTSREKEVLQWCAIGKTSWEISVICNCSEANVNFHMGNIRRKFGVTSRRVAAIMAVNLGLITL
QscR     SMLSLVRSSESIAAT-EILEKESFLLWITSMLQATFGDLLAPRIVPESNVRLTARETEMLKWTAVGKTYGEIGLILSIDQRTVKFHIVNAMRKLNSSNKAEATMKAYAIGLLN-
```

SUPPLEMENTAL COMPOUND CHARACTERIZATION DATA

3-hydroxy-hexadecanoyl-L-homoserine lactone (15). *Mixture of diastereomers*. ^{1}H NMR (500 MHz, $CDCl_3$) δ 6.49 (apparent dd, *J* = 30.7, 6.0 Hz, 1H), 4.56 (ddt, *J* = 11.7, 8.6, 6.4 Hz, 1H), 4.51–4.45 (m, 1H), 4.29 (ddd, *J* = 11.3, 9.3, 5.9 Hz, 1H), 4.02 (dtd, *J* = 9.6, 4.8, 2.3 Hz, 1H), 2.87–2.79 (m, 1H), 2.45 (ddd, *J* = 15.4, 11.5, 2.7 Hz, 1H), 2.34 (ddd, *J* = 15.5, 10.7, 9.1 Hz, 1H), 2.18 (qdd, *J* = 11.7, 8.8, 4.9 Hz, 1H), 1.92–1.10 (m, 27H, 3 protons high due to small grease contamination), 0.88 (t, *J* = 6.9 Hz, 3H); ^{13}C NMR (126 MHz, $CDCl_3$) δ 175.39, 175.38, 173.09, 173.04, 68.80, 68.74, 66.23, 66.21, 49.40, 49.34, 42.61, 37.15, 37.04, 32.08, 30.53, 30.50, 29.84, 29.83, 29.81, 29.73, 29.72, 29.64, 29.51, 25.62, 25.59, 22.85, 14.28; ESI-MS: expected m/z = 356.28, observed 356.28 $[M+H]^+$.

3-hydroxy-4-(3-chloro-phenyl)butanoyl-L-homoserine lactone (22). *Mixture of diastereomers*. ^{1}H NMR (500 MHz, DMSO-*d*6) δ 8.38 (d, *J* = 7.9 Hz, 1H), 8.35 (d, *J* = 8.1 Hz, 1H), 7.34–7.22 (m, 6H), 7.21–7.13 (m, 2H), 4.85 (dd, *J* = 5.5, 3.2 Hz, 2H), 4.59 (dt, *J* = 10.9, 8.6 Hz, 1H), 4.49 (dt, *J* = 10.6, 8.5 Hz, 1H), 4.34 (td, *J* = 8.9, 1.7 Hz, 2H), 4.20 (dddd, *J* = 11.1, 9.1, 6.4, 2.7 Hz, 2H), 4.05 (p, *J* = 5.1 Hz, 2H), 2.75 (dt, *J* = 13.6, 3.7 Hz, 2H), 2.62 (ddd, *J* = 13.5, 7.4, 3.9 Hz, 2H), 2.42–2.33 (m, 2H), 2.28–2.07 (m, 6H); ^{13}C NMR (126 MHz, DMSO-*d*6) δ 175.82, 171.02, 142.22, 133.03, 130.26, 129.74, 128.70, 126.32, 68.71, 65.74, 48.42, 48.21, 43.37, 43.29, 42.76, 42.74, 28.74, 28.64; ESI-MS: expected m/z = 297.08, observed 320.2 $[M+Na]^+$.

3-hydroxy-4-(3-iodo-phenyl)butanoyl-L-homoserine lactone (23). *Mixture of diastereomers*. ^{1}H NMR (500 MHz, $CDCl_3$) δ 7.54–7.50 (m, 2H), 7.15–7.10 (m, 1H), 6.98 (t, *J* = 7.9 Hz, 1H), 6.41 (apparent dd, *J* = 17.6, 6.1 Hz, 1H), 4.48 (ddt, *J* = 11.5, 8.5, 6.7 Hz, 1H), 4.41 (tt, *J* = 8.5, 1.3 Hz, 1H), 4.26–4.14 (m, 2H), 2.79–2.63 (m, 3H), 2.43–2.25 (m, 2H), 2.11 (qdd, *J* = 11.8, 8.8, 6.1 Hz, 1H); ^{13}C NMR (126 MHz, $CDCl_3$) δ 175.18, 175.17, 172.40, 172.36, 139.93, 139.92, 138.34, 135.88, 130.34, 128.78, 128.76, 94.66, 69.25, 69.18, 66.09, 66.07, 49.24, 49.21, 42.76, 42.59, 41.55, 41.53, 30.24, 30.21; ESI-MS: expected m/z = 389.01, observed 411.7 $[M+Na]^+$.

3-oxo-4-(3-iodo-phenyl)butanoyl-L-homoserine lactone (26). *Keto and enol tautomers present*. ^{1}H NMR (500 MHz, $CDCl_3$) δ 13.29 (s, 0.14H, enol), 7.67–7.59 (m, 1H), 7.57 (d, *J* =

1.8 Hz, 1H), 7.39 (d, *J* = 6.4 Hz, 0.83H, keto), 7.24–7.15 (m, 1H), 7.08 (dt, *J* = 12.5, 7.9 Hz, 1H), 5.65 (d, *J* = 5.8 Hz, 0.12H, enol), 4.77 (s, 0.14H, enol), 4.56 (ddd, *J* = 11.6, 8.7, 6.4 Hz, 1H), 4.47 (td, *J* = 9.1, 1.4 Hz, 1H), 4.27 (ddd, *J* = 11.2, 9.3, 6.0 Hz, 1H), 3.76 (s, 1.67H, keto), 3.51 (s, 1.68H, keto), 3.42 (s, 0.27H, enol), 2.84 (ddd, *J* = 13.5, 8.5, 6.0 Hz, 0.16H, enol), 2.76 (dddd, *J* = 12.6, 8.7, 6.0, 1.3 Hz, 0.88H, keto), 2.27–2.14 (m, 1H); ^{13}C NMR (126 MHz, $CDCl_3$) δ 203.03, 174.74, 165.95, 138.58, 136.85, 134.96, 130.71, 128.99, 94.87, 66.03, 50.04, 49.30, 47.81, 30.05; ESI-MS: expected m/z = 387.00, observed 409.7 $[M+Na]^+$.

NMR spectra for compounds 15, 22, 23, and 26.

15:

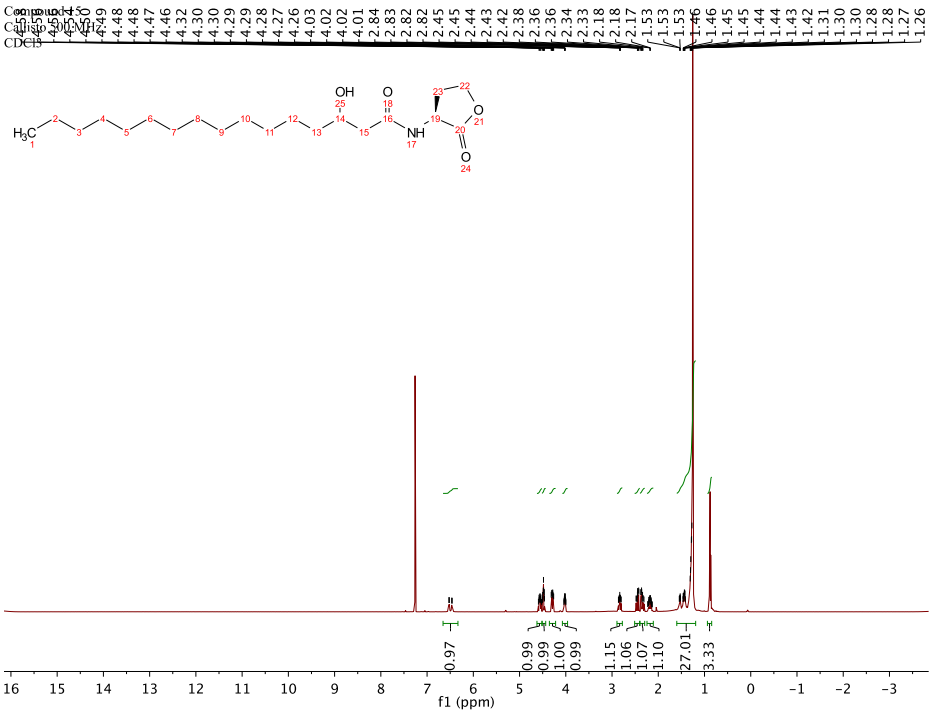

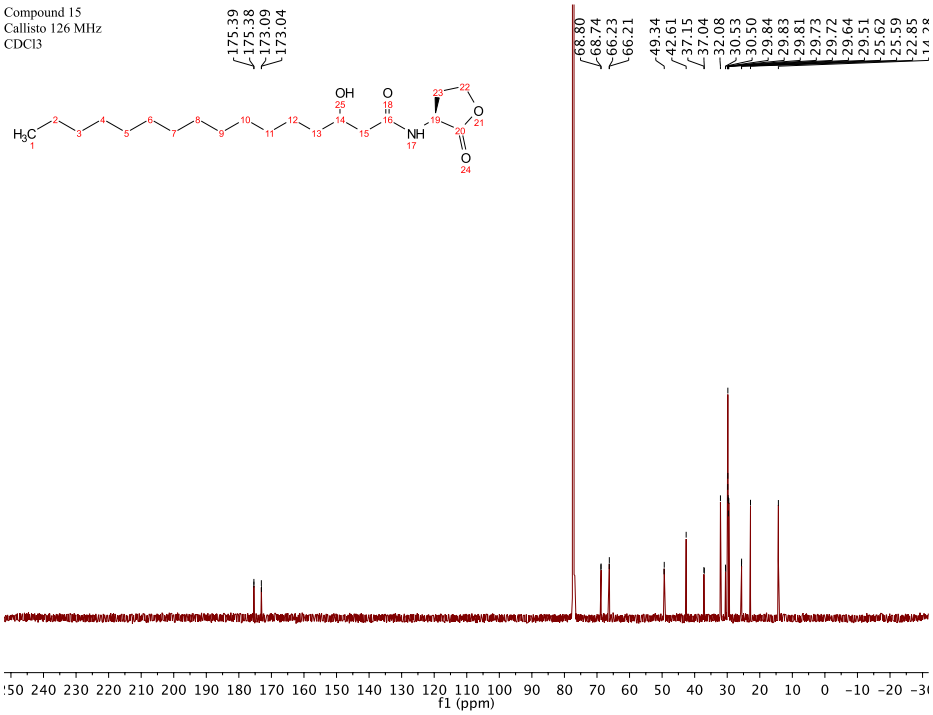

22:

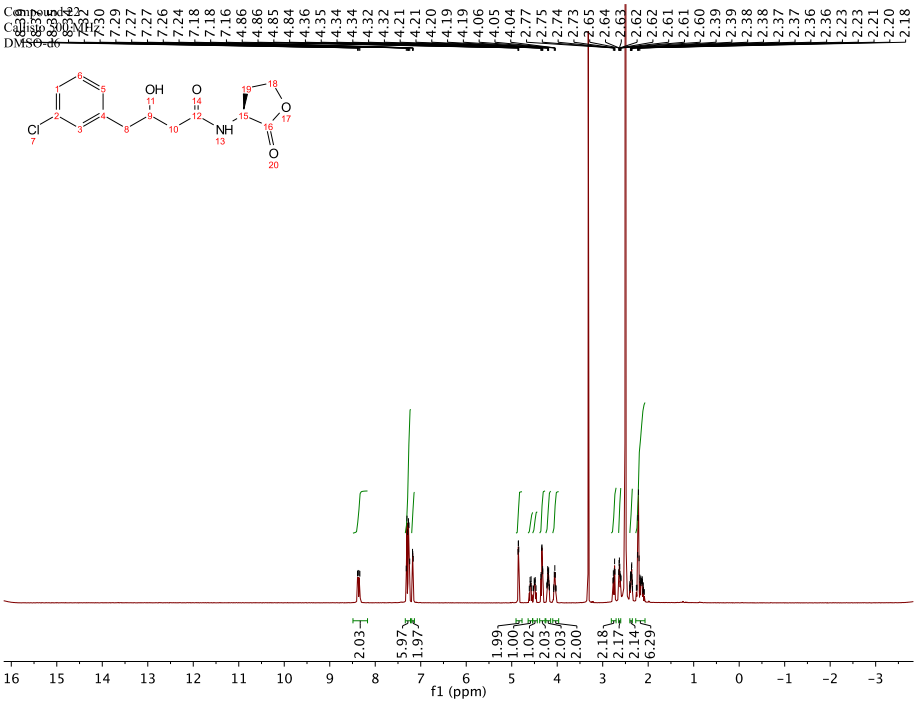
Compound 22
Callisto 126 MHz
DMSO-d6
f1 (ppm)

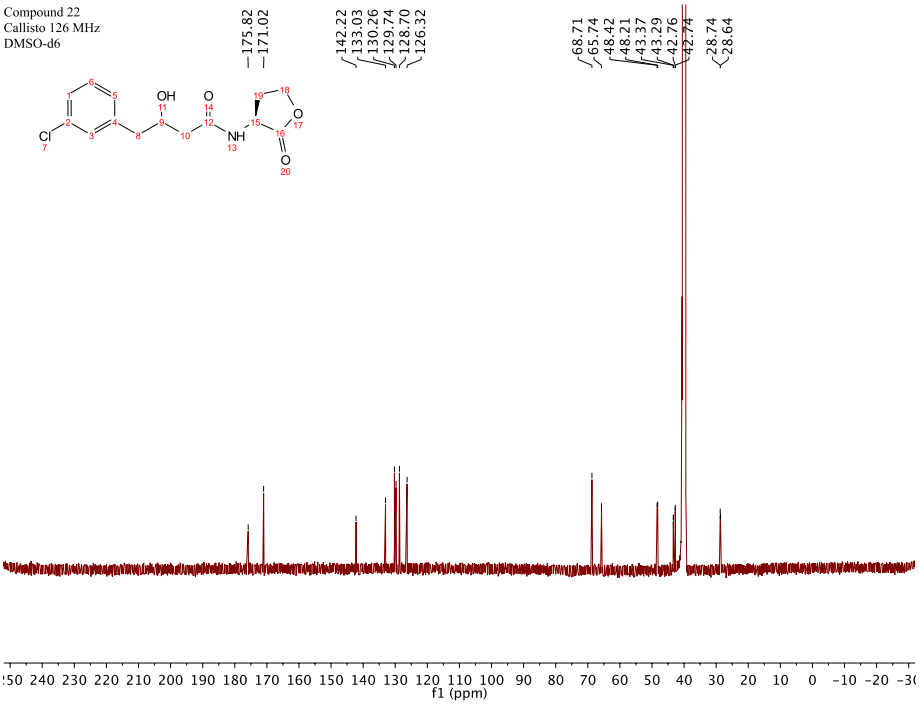
Compound 22
Callisto 126 MHz
DMSO-d6
175.82
171.02
142.22
133.03
130.26
129.74
128.70
126.32
68.71
65.74
48.42
48.21
43.37
43.29
42.76
42.74
28.74
28.64
f1 (ppm)

23:

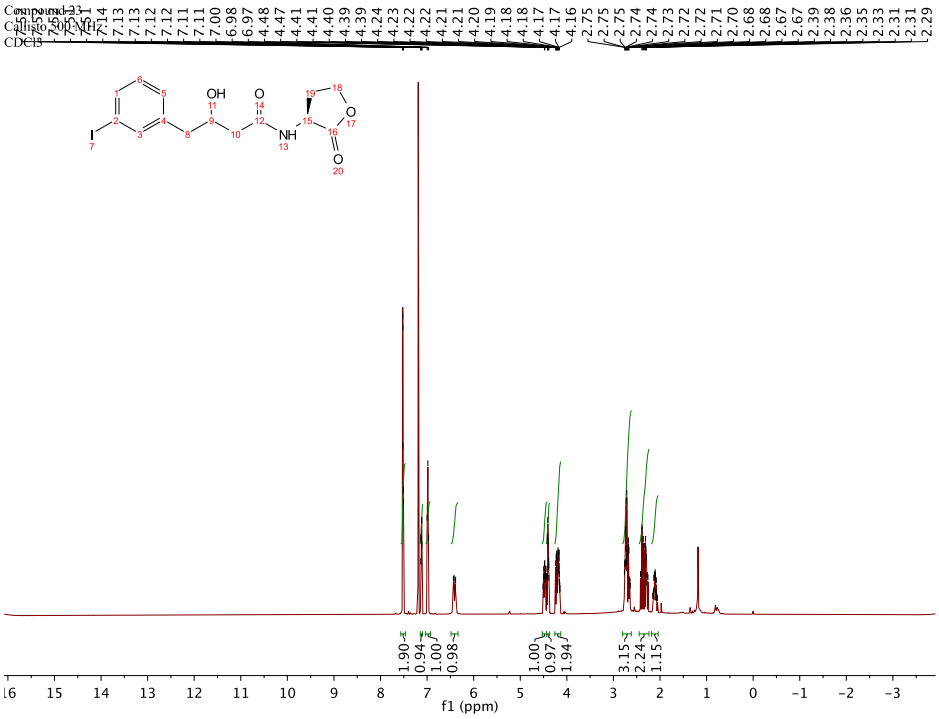
Compound 23
Callisto 700 MHz
CDCl3
f1 (ppm)

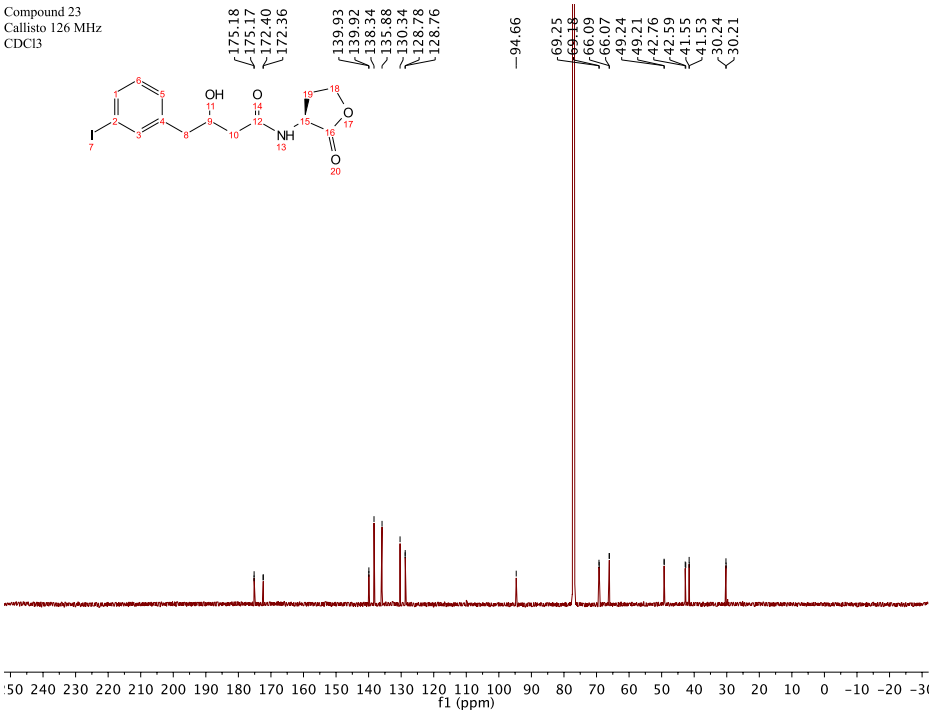
Compound 23
Callisto 126 MHz
CDCl3
f1 (ppm)

26:

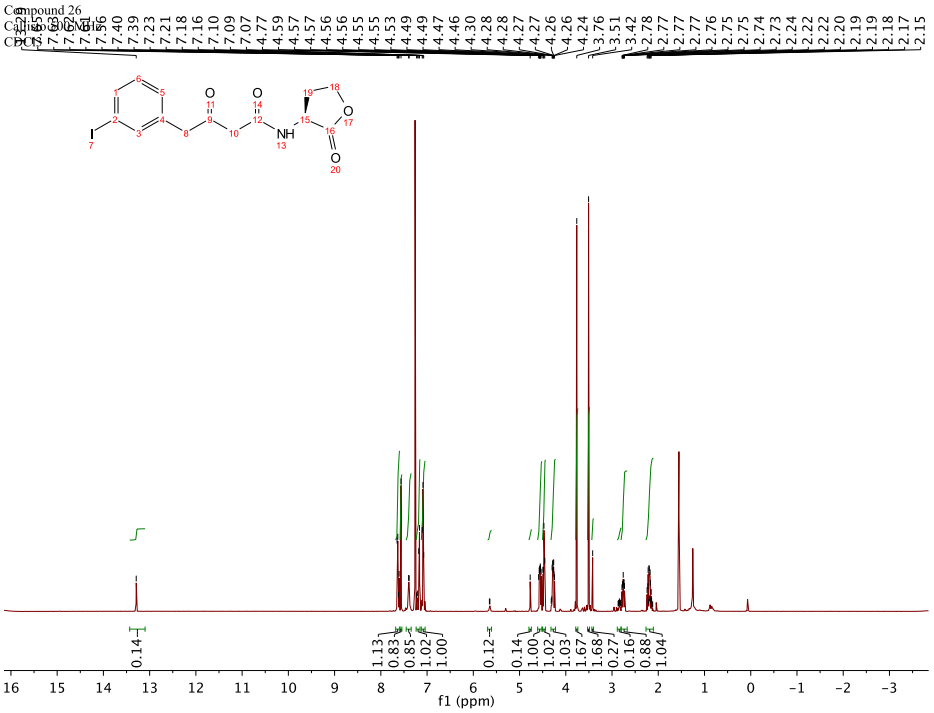
Compound 26
Callisto 126 MHz
CDCl3
f1 (ppm)

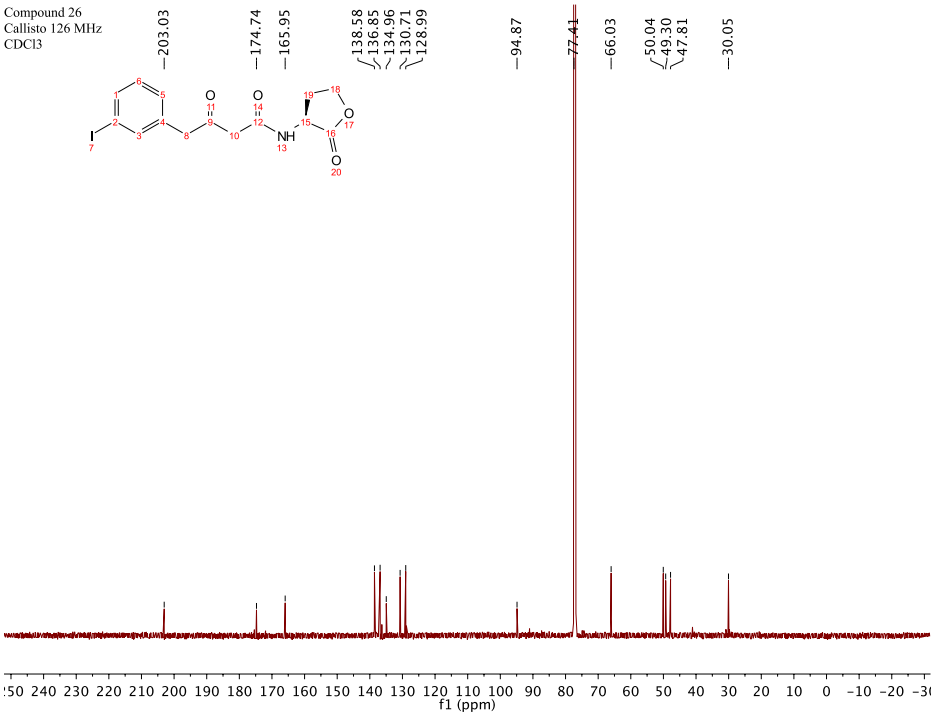
Compound 26
Callisto 126 MHz
CDCl3
203.03
174.74
165.95
138.58
136.85
134.96
130.71
128.99
94.87
77.41
66.03
50.04
49.30
47.81
30.05
f1 (ppm)

REFERENCES

1. Geske, G. D., O'Neill, J. C., Miller, D. M., Mattmann, M. E., and Blackwell, H. E. (2007) Modulation of bacterial quorum sensing with synthetic ligands: systematic evaluation of *N*-acylated homoserine lactones in multiple species and new insights into their mechanisms of action, *J. Am. Chem. Soc. 129*, 13613-13625.

2. Geske, G. D., ONeill, J. C., Miller, D. M., Wezeman, R. J., Mattmann, M. E., Lin, Q., and Blackwell, H. E. (2008) Comparative analyses of *N*-acylated homoserine lactones reveal unique structural features that dictate their ability to activate or inhibit quorum sensing, *ChemBioChem 9*, 389-400.

3. Stacy, D. M., Welsh, M. A., Rather, P. N., and Blackwell, H. E. (2012) Attenuation of quorum sensing in the pathogen *Acinetobacter baumannii* using non-native *N*-acyl homoserine lactones, *ACS Chem. Biol. 7*, 1719-1728.

4. Mcinnis, C. E., and Blackwell, H. E. (2011) Design, synthesis, and biological evaluation of abiotic, non-lactone modulators of LuxR-type quorum sensing, *Bioorg. Med. Chem. 19*, 4812-4819.

5. Mcinnis, C. E., and Blackwell, H. E. (2011) Thiolactone modulators of quorum sensing revealed through library design and screening, *Bioorg. Med. Chem. 19*, 4820-4828.

6. Miller, J. H. (1972) *Experiments in Molecular Genetics*, Cold Spring Press, Plainview, NY.

7. Niu, C., Clemmer, K. M., Bonomo, R. A., and Rather, P. N. (2008) Isolation and characterization of an autoinducer synthase from *Acinetobacter baumannii*, *J. Bacteriol. 190*, 3386-3392.

8. Lee, J.-H., Lequette, Y., and Greenberg, E. P. (2006) Activity of purified QscR, a *Pseudomonas aeruginosa* orphan quorum-sensing transcription factor, *Mol. Microbiol. 59*, 602-609.

9. Stacy, D. M., Welsh, M. A., Rather, P. N., and Blackwell, H. E. (2012) Attenuation of quorum sensing in the pathogen *Acinetobacter baumannii* using non-native *N*-acyl homoserine lactones, *ACS Chem. Biol. 7*, 1719-1728.

10. Reverchon, S., Chantegrel, B., Deshayes, C., Doutheau, A., and Cotte-Pattat, N. (2002) New synthetic analogues of *N*-acyl homoserine lactones as agonists or antagonists of transcriptional regulators involved in bacterial quorum sensing, *Bioorg. Med. Chem. Lett. 12*, 1153-1157.

11. McClean, K. H., Winson, M. K., Fish, L., Taylor, A., Chhabra, S. R., Camara, M., Daykin, M., Lamb, J. H., Swift, S., Bycroft, B. W., Stewart, G. S., and Williams, P. (1997) Quorum sensing and *Chromobacterium violaceum*: exploitation of violacein production and inhibition for the detection of *N*-acylhomoserine lactones, *Microbiology 143*, 3703-3711.

12. Flavier, A. B., Ganova-Raeva, L. M., Schell, M. A., and Denny, T. P. (1997) Hierarchical autoinduction in *Ralstonia solanacearum*: control of acyl-homoserine lactone production by a novel autoregulatory system responsive to 3-hydroxypalmitic acid methyl ester, *J. Bacteriol. 179*, 7089-7097.

13. Laue, B. E., Jiang, Y., Chhabra, S. R., Jacob, S., Stewart, G. S., Hardman, A., Downie, J. A., O'gara, F., and Williams, P. (2000) The biocontrol strain *Pseudomonas fluorescens* F113 produces the *Rhizobium* small bacteriocin, *N*-(3-hydroxy-7-cis-tetradecenoyl)homoserine lactone, via HdtS, a putative novel *N*-acylhomoserine lactone synthase, *Microbiology 146*, 2469-2480.

14. Lewenza, S., Conway, B., Greenberg, E. P., and Sokol, P. A. (1999) Quorum sensing in *Burkholderia cepacia*: identification of the LuxRI homologs CepRI, *J. Bacteriol. 181*, 748-756.

15. Teplitski, M., Mathesius, U., and Rumbaugh, K. P. (2011) Perception and degradation of *N*-acyl homoserine lactone quorum sensing signals by mammalian and plant cells, *Chem. Rev. 111*, 100-116.

16. Cataldi, T. R. I., Bianco, G., Palazzo, L., and Quaranta, V. (2007) Occurrence of *N*-acyl-l-homoserine lactones in extracts of some Gram-negative bacteria evaluated by gas chromatography–mass spectrometry, *Anal. Biochem. 361*, 226-235.

17. Schaefer, A. L., Taylor, T. A., Beatty, J. T., and Greenberg, E. P. (2002) Long-chain acyl-homoserine lactone quorum-sensing regulation of *Rhodobacter capsulatus* gene transfer agent production, *J. Bacteriol. 184*, 6515-6521.

18. Gao, M., Chen, H., Eberhard, A., Gronquist, M. R., Robinson, J. B., Rolfe, B. G., and Bauer, W. D. (2005) *sinI*- and *expR*-dependent quorum sensing in *Sinorhizobium meliloti*, *J. Bacteriol. 187*, 7931-7944.

19. Savka, M. A., Le, P. T., and Burr, T. J. (2010) LasR receptor for detection of long-chain quorum-sensing signals: identification of *N*-acyl-homoserine lactones encoded by the *avsI* locus of *Agrobacterium vitis*, *Curr. Microbiol. 62*, 101-110.

20. Mao, D., Bushin, L. B., Moon, K., Wu, Y., and Seyedsayamdost, M. R. (2017) Discovery of *scmR* as a global regulator of secondary metabolism and virulence in *Burkholderia thailandensis* E264, *Proc. Natl. Acad. Sci. U. S. A. 114*, E2920-E2928.

21. Thiel, V., Kunze, B., Verma, P., Wagner-Döbler, I., and Schulz, S. (2009) New structural variants of homoserine lactones in bacteria, *ChemBioChem 10*, 1861-1868.

22. Berger, M., Neumann, A., Schulz, S., Simon, M., and Brinkhoff, T. (2011) Tropodithietic acid production in *Phaeobacter gallaeciensis* is regulated by *N*-acyl homoserine lactone-mediated quorum sensing, *J. Bacteriol. 193*, 6576-6585.

23. Duerkop, B. A., Herman, J. P., Ulrich, R. L., Churchill, M. E. A., and Greenberg, E. P. (2008) The *Burkholderia mallei* BmaR3-BmaI3 quorum-sensing system produces and responds to *N*-3-hydroxy-octanoyl homoserine lactone, *J. Bacteriol. 190*, 5137-5141.

24. Myszka, K., Olkowicz, M., Radziejewska-Kubzdela, E., Olejnik-Schmidt, A. K., and Czaczyk, K. (2015) Impact of bacterial quorum sensing system on changes of organoleptic markers of storage cabbage, *J. Microbiol., Biotechnol. Food Sci. 4*, 407-411.

25. Eberhard, A., Burlingame, A. L., Eberhard, C., Kenyon, G. L., Nealson, K. H., and Oppenheimer, N. J. (1981) Structural identification of autoinducer of *Photobacterium fischeri* luciferase, *Biochemistry 20*, 2444-2449.

26. Steidle, A., Sigl, K., Schuhegger, R., Ihring, A., Schmid, M., Gantner, S., Stoffels, M., Riedel, K., Givskov, M., Hartmann, A., Langebartels, C., and Eberl, L. (2001) Visualization of *N*-acylhomoserine lactone-mediated cell-cell communication between bacteria colonizing the tomato rhizosphere, *Appl. Environ. Microbiol. 67*, 5761-5770.

27. Fuqua, W. C., and Winans, S. C. (1994) A LuxR-LuxI type regulatory system activates *Agrobacterium* Ti plasmid conjugal transfer in the presence of a plant tumor metabolite, *J. Bacteriol. 176*, 2796-2806.

28. Milton, D. L., Hardman, A., Camara, M., Chhabra, S. R., Bycroft, B. W., Stewart, G. S., and Williams, P. (1997) Quorum sensing in *Vibrio anguillarum*: characterization of the *vanI*/*vanR* locus and identification of the autoinducer *N*-(3-oxodecanoyl)-L-homoserine lactone, *J. Bacteriol. 179*, 3004-3012.

29. Pearson, J. P., Gray, K., Passador, L., and Tucker, K. (1994) Structure of the autoinducer required for expression of *Pseudomonas aeruginosa* virulence genes, *Proc. Natl. Acad. Sci. U. S. A. 91*, 197-201.

30. Wong, C.-S., Yin, W.-F., Choo, Y.-M., Sam, C.-K., Koh, C.-L., and Chan, K.-G. (2011) Coexistence of quorum-quenching and quorum-sensing in tropical marine *Pseudomonas aeruginosa* strain MW3A, *World J. Microbiol. Biotechnol. 28*, 453-461.

31. Chang, C.-Y., Koh, C.-L., Sam, C.-K., Chan, X.-Y., Yin, W.-F., and Chan, K.-G. (2012) Unusual long-chain *N*-acyl homoserine lactone production by and presence of quorum quenching activity in bacterial isolates from diseased tilapia fish, *PLoS ONE 7*, e44034-44038.